

This is the Submitted Manuscript version of an article accepted for publication in Catalysis Today. Elsevier is not responsible for any errors or omissions in this version of the manuscript or any version derived from it. The Version of Record is available online at <https://doi.org/10.1016/j.cattod.2014.04.021>

UV AND SOLAR-BASED PHOTOCATALYTIC DEGRADATION OF ORGANIC POLLUTANTS BY NANO-SIZED TiO₂ GROWN ON CARBON NANOTUBES

S. Murgolo¹, F. Petronella², R. Ciannarella¹, R. Comparelli², A. Agostiano^{2,3}, M. L. Curri²,
G. Mascolo^{1*}

(1) CNR, Istituto di Ricerca Sulle Acque, Via F. De Blasio 5, 70132 Bari, Italy

(2) CNR, Istituto per i Processi Chimico-Fisici, Via Orabona 4, 70126 Bari, Italy

(3) Dipartimento di Chimica Università degli Studi di Bari, Via Orabona 4, 70126 Bari, Italy

* Corresponding author. Tel.: +39 080 5820519; fax: +39 080 5313365.

E-mail address: giuseppe.mascolo@ba.irsacnr.it (G. Mascolo).

Abstract

A new photocatalyst based on nano-sized TiO₂ supported on single wall carbon nanotubes (SWCNTs) with tailored photocatalytic properties upon irradiation by both UV and solar simulated light was successfully employed for the degradation of a mixture of 22 organic pollutants in both ultrapure water and secondary wastewater effluent. First-order degradation rates showed that under UV irradiation nano-sized TiO₂ supported on SWCNTs is much more effective than conventional Degussa P25 for degradation of iopamidol, iopromide, diatrizoic acid, diclofenac, triclosan and sulfamethoxazole in ultrapure water. For the remaining organics the degradation rates were comparable being in most of the cases Degussa P25 slightly more effective than nano-sized TiO₂ supported on SWCNTs. Reactions performed in secondary wastewater effluent showed a general reduction of degradation rates. Specifically, such a reduction was in the range 9-87 % and 9-96 % for the Degussa P25 and the nano-sized TiO₂ supported on SWCNTs, respectively. Overall, the nano-sized TiO₂ supported on SWCNTs under UV irradiation displayed comparable degradation rates with respect to convention Degussa P25. Under simulated solar irradiation the new prepared photocatalyst showed lower efficiency than Degussa P25 in ultrapure water. Such a gap was greatly reduced when the reactions were carried out in real secondary wastewater effluent. The nano-sized TiO₂ supported on SWCNTs demonstrated to have the addition benefit to be easily removed from the aqueous solution by a mild centrifugation or a filtration step and, consequently, can be reused for a further photocatalytic treatment batch. Therefore, the obtained results showed that new photocatalyst based on nano-sized TiO₂ supported on SWCNTs has proved to be a promising candidate to be used in a photocatalytic based-AOP and to be integrated with a biological step for the effective removal of emerging organic pollutants.

Keywords

photocatalysis, TiO₂ nanoparticles, PPCPs, carbon nanotubes, recalcitrant pollutants.

1. Introduction

Conventional wastewater treatment plants (WWTPs) that are typically based on biological processes where wastewater is treated by an activated sludge, have been designed to remove/decrease conventional pollution parameters such as BOD₅, COD, total suspended solid, etc. Nevertheless such plants are not able to completely remove a wide variety of persistent, toxic and/or not biodegradable organic pollutants as well as pharmaceuticals and personal care products (PPCPs) [1-3]. Therefore,

most of the aforementioned organics end up in the receiving water bodies and, consequently, WWTPs are nowadays considered as secondary sources of pollutants discharged into environment [4, 5]. In fact, PPCPs have been even found in drinking water, with concentrations ranging from ng L^{-1} to $\mu\text{g L}^{-1}$ [1, 6, 7] with also evident negative effects on aquatic organisms [8, 9]. Such organic pollutants have been recently classified as “emerging contaminants” as they are still unregulated, although likely to be included in future environmental legislation, on the basis of the results research activities reporting their adverse effects towards flora, fauna, and humans due to their biological potency [2]. In addition, human health concerns on PPCPs are particularly serious in regions where an indirect potable reuse can occur. Indirect potable reuse can take place through recharge of unconfined or confined aquifers, via surface spreading or direct injection, or by surface water augmentation into a stream or reservoir that serves as a source for drinking water [10]. PPCPs as well as endocrine disruptor compounds (EDCs), pesticides, and other xenobiotic substances [1] are known to enter the environment through individual anthropic activities and as residue from pharmaceutical industry, agribusiness, veterinary use, and hospitals and community use [2, 3]. Currently, most of the research activities in the field are therefore oriented towards the development of innovative and effective technologies applicable in full scale for the removal of emerging organic pollutants in water. In this perspective, advanced oxidation processes (AOPs) have been identified as a promising technology for degrading such compounds [2, 6, 11]. AOPs are generally defined as oxidation methods based on the action of highly reactive and unselective species such as hydroxyl radicals, the second highest known oxidant species ($E^0=2.81 \text{ V}$), which are able to promote organic matter oxidation and mineralization at high reaction rates [7]. Although the treatment of wastewater is far the most common area for research and development, AOPs have found also several other applications such as groundwater treatment, soil remediation, ultrapure water production, treatment of organic volatile compounds and odor control.

Among AOPs, the most common techniques include ozone-based processes ($\text{O}_3/\text{H}_2\text{O}_2$, O_3/UV) [12], photochemical processes ($\text{UV}/\text{H}_2\text{O}_2$, O_3/UV) [13], Fenton and photo-Fenton ($\text{H}_2\text{O}_2/\text{Fe}^{2+}$, $\text{H}_2\text{O}_2/\text{Fe}^{2+}/\text{UV}$) and photocatalysis [14]. Heterogeneous photocatalysis assisted by titanium dioxide (TiO_2), in anatase and rutile crystallites, is one of the most attractive, being an environmental friendly and sustainable technology since no chemicals are employed. TiO_2 is the most widely investigated photocatalyst due to high photo-activity, low cost, low toxicity and good chemical and thermal stability [15-17]. Irradiation of TiO_2 promotes the transition of an electron from the full valence band to the empty conduction band. In order to promote electron excitation, the adsorbed photon must have an energy equal or higher than TiO_2 band gap (3.2 eV for anatase, 3.0 eV for rutile and $\sim 3.2 \text{ eV}$ for brookite) [18]. This mechanism generates electron (e_{CB}^-) – hole (h_{VB}^+) pairs which lead to a sequence

of redox reaction responsible for the organic degradation of contaminants [19, 20]. Typically, such a mechanism involves the oxidation of adsorbed H₂O by photogenerated holes and reduction of an electron acceptor (typically dissolved oxygen) by photoexcited electrons. These reactions lead to the production of a hydroxyl and superoxide radicals anion that can subsequently oxidize organic species up to mineralization, i.e. producing mineral salts, CO₂ and H₂O. However, AOPs are known to lead to degradation products in the common practice of water treatment, namely when employing reaction time in the range of 5-30 min [21-25].

The conventional photocatalyst TiO₂ Degussa P25 is generally used in aqueous suspension in order to exploit the maximum available active surface. However, the micrometric size of the particles makes the photocatalyst difficult to be recovered at the end of the treatment and to be recycled. Such disadvantage represents a substantial limitation for the scale-up of the process. Another significant problem is given by the “shadowing effect”, that the suspension of the photocatalyst exerts against the radiation that activates the process itself ultimately resulting in a reduced irradiation intensity. Several efforts have been made to overcome these drawbacks, and particularly to immobilize photocatalysts onto substrates, such as glass beads, glass fibres, silica, stainless steel, textiles, honeycombs, activated carbon, and zeolites [26-29]. Therefore, the design and implementation of novel TiO₂-based photocatalysts deposited onto suitable substrates to obtain materials exploitable for specifically addressing environmental applications, is a challenging task. In this framework, the heterogeneous photocatalysis assisted by supported TiO₂ is considered a tertiary treatment process in a conventional wastewater treatment plant applicable after or in combination with biological step without any drawback for biomass [30]. The photocatalyst, indeed, can be thus separated from the reaction solution and possibly recycled without the addition of any reagent such as H₂O₂ or iron salts. However, the immobilization of the photocatalyst inevitably leads to a loss of photocatalytic efficiency because its active surface is reduced once deposited onto a surface. In this context an innovation is represented by nanostructured photocatalysts. Nano-sized TiO₂ are expected to reduce such loss of performance due to their extremely high surface-to-volume ratio, which greatly increases the density of active sites available for adsorption and catalysis. Moreover, the size-dependent band gap allows to tune the electron-hole redox potentials and thus to control selectivity in photochemical reactions. The small size of the nanophotocatalysts allows also the photo-generated charges to readily migrate on the photocatalyst surface thus reducing the probability of undesired bulk recombination. Carbon nanotube represents an appealing alternative to substrates commonly used for photocatalyst immobilization since they can simultaneously provide (i) easy photocatalyst recovery, owing to their micrometric size, (ii) retardation of electron-hole pair recombination and (iii) visible light catalysis by modification of band-gap [31].

Indeed, a common drawback of AOPs is the high demand of electrical energy for devices such as ozonizers, UV lamps, ultrasounds, which results in rather high treatment costs. Solar-based AOPs seem to be very promising due to their capability of working even with visible light, leading to a reduction of the operating costs of large-scale aqueous-phase applications [32, 33]. Solar driven photo-Fenton should be preferred from an integrated environmental and economic point of view, considering a comparison between several AOPs for wastewater treatment regarding their life-cycle greenhouse gas emissions and life-cycle cost [21]. Recent papers have reported that emerging pollutants, in mixture at low concentration ($\mu\text{g L}^{-1}$ range), can be successfully removed in wastewater treatment plants effluents reaching a negligible concentration with solar photo-Fenton [34-36]. In addition, most of the literature reports on photocatalysis processes performed under ideal conditions that cannot be easily transferred to practical applications. Specifically, most experimental studies include reaction kinetics of individual contaminants in the absence of constituents that are typically present in real water matrices at orders-of-magnitude higher concentration.

The present work reports about the degradation of a mixture of 22 PPCPs and EDCs at low concentration ($\mu\text{g L}^{-1}$ range) by means of a photocatalysis process based on a new photocatalyst formed of nano-sized TiO_2 grown onto single wall carbon nanotubes (SWCNTs).

Such an innovative material, based on an in situ synthesis of anatase TiO_2 nanoparticles at the surface of SWCNT, offers the unique chance of combining the widely assessed photocatalytic activity of the nanostructured TiO_2 with the outstanding electronic behaviour of SWCNTs, in one original composite structure.

The main objectives of the study were (i) to investigate direct photolysis and photocatalysis employing the new nano-sized TiO_2 photocatalyst with UV and simulated solar light; (ii) to compare the efficiency of the new prepared nanostructured photocatalyst with respect to the conventional TiO_2 Degussa P25 photocatalyst; (iii) to evaluate the influence of the water matrix (secondary effluent of municipal WWTP) on the photolysis and photocatalytic kinetics of the investigated PPCPs.

2. Materials and methods

2.1 Chemicals and wastewater effluent

Chemicals and solvents used for chromatographic analyses and for preparing standard solutions, methanol, ammonium acetate were HPLC grade (Riedel-de Haën, Baker). Ultrapure water (18.2 M Ω cm, organic carbon $\leq 4\mu\text{g/L}$) was obtained by a Milli-Q Gradient A-10 (Millipore) system and employed for ultra-high pressure liquid chromatography (UPLC). Chemical structure and main

information of the 22 selected PPCPs and EDCs (Sigma-Aldrich) are displayed in Table 1. Stock aqueous solutions were prepared in MilliQ water. Synthetic amorphous titanium dioxide Degussa (Evonik) P25 (anatase and rutile crystallites with ratio being typically 80:20, surface area 50 m²/g, average diameter 30 nm) was employed [23]. For actinometry experiments uridine (Sigma-Aldrich) was employed.

Titanium tetraisopropoxide (TTIP, 99.999%), trimethylamino-N-oxide dihydrate (TMAO, 98%), and oleic acid (OLEA, 90%), SWCNTs (50-70%) were purchased from Sigma-Aldrich. All chemicals were of the highest purity available and were used as received without further purification. All solvents used were of analytical grade and purchased from Aldrich.

The real secondary effluent was taken from a laboratory scale plant, namely a SBBGR system (Sequencing Batch Biofilter Granular Reactor) used for the treatment of urban wastewater [37]. The secondary effluent was firstly characterized and then filtered to remove coarse material (algae and various residues arising from the reactor), which can cause interference in photodegradation reactions. The main characteristics of the secondary effluent used are listed in Table 2.

2.2 Nano-sized SWCNTs/TiO₂ photocatalyst synthesis

Rod-like TiO₂ nanocrystals were synthesized in anatase phase by suitably modifying a reported approach exploiting the hydrolysis of TTIP catalyzed by TMAO dihydrate in presence of OLEA at 100°C [38]. The synthetic procedure was carried out at the surface of SWCNT, by using standard airless techniques. 2.3 mg of SWCNT was dispersed in 70 g of OLEA by sonication for 15 min. The obtained dispersion was kept under vacuum at 100 °C for 15 min under vigorous stirring. Under nitrogen flow, 16 mmol of TTIP was added and the solution turned from colorless to pale yellow. At this stage, 5 mL of a 1 M aqueous solution of TMAO dihydrate was rapidly injected into the reaction mixture. The solution was maintained in a closed system at 100 °C and stirred under mild reflux with water over 5 days to promote further hydrolysis and crystallization of the product. The reaction was stopped by removing heating and a grey powder recovered by adding ethanol or methanol. The SWCNTs/TiO₂ NRs heterostructure was then dispersed in apolar organic solvents as CHCl₃, or hexane. Prior to photocatalytic tests, the excess of surfactant has been removed by repeatedly washing with CHCl₃/methanol and subsequent centrifugation and the collected grey powder has been dried under vacuum overnight.

Total amount of TiO₂ deposited onto the supporting nanotubes was determined by mineralizing a small amount of photocatalyst (about 1 g) and then determining the Ti concentration of the obtained acidic solutions using a 7700x (Agilent) inductively coupled plasma mass spectrometer. It was found that the TiO₂ concentration is 0.58 mg_{TiO₂}/mg_{SWCNTs}.

2.3 Analytical determinations

The residual concentration of the investigated compounds at various reaction time was determined by UPLC/MS-MS analysis by an Acquity chromatographic system, equipped with both an auto-sampler and a photo-diode array detector (Waters), interfaced to an API 5000 mass spectrometer (AB Sciex) by means of a ESI or APCI depending on the chemical characteristics of the organic pollutants. The analytical conditions, including source and ionization mode were firstly defined for each analyte by using positive/negative ESI and APCI through direct infusion into the mass spectrometer. Secondly, the optimal source-dependent parameters (Table S1 of the supporting information) and compound-dependent parameters (Table S2 of the supporting information) were determined using that source/polarity. Based on the obtained results, a multi-residue method for the simultaneous determination of selected organic pollutants in water samples was developed. The mass analysis was performed in multiple reaction monitoring mode employing proper mass transitions (Figure S1 and S2 of the supporting information). 5 μ L samples were injected by a Rheodyne valve equipped with a 10 μ L loop, and eluted at 0.050 mL/min through a BEH C18 column, 1.0 x 150 mm, 1.7 μ m, with a binary gradient consisting of 1.5 mM ammonium in water (A) and 1.5 mM ammonium in methanol (B). The gradient was as follows: 20 % B at the initial point, linearly increased to 80 % in 10 min and held for 7 min. A 7 min equilibration step at 20 % B was used at the end of each run to bring the total run time per sample to 24 minutes.

Transmission electron microscopy (TEM) analysis was performed by a JEOL JEM-1011 microscope operating at 100kV. The TEM samples were prepared by casting a drop of SWCNTs/TiO₂.CHCl₃ solution onto a carbon hollowed TEM grid.

Field emission scanning electron microscopy (FE-SEM) was performed by a Zeiss Sigma microscope operating in the range 0.5-20kV and equipped with an in-lens secondary electron detector. FE-SEM samples were prepared by casting a few drop of SWCNTs/TiO₂ CHCl₃ solution onto a silicon slide. Samples were mounted onto stainless-steel sample holders by using double-sided carbon tape and grounded by silver paste.

2.4 Laboratory-scale experiments

A 0.6 L cylindrical Pyrex glass reactor was used for performing degradation experiments, in batch mode. A low pressure 17 W mercury arc lamp (Helios Italquartz, Italy) emitting at 254 nm was employed as UV radiation source for UV/TiO₂ experiments. The low pressure UV lamp was characterized by actinometry (uridine) obtaining a flow rate of 0.10 W/cm². In a typical experimental test 500 mL of a solution of the selected organic pollutants freshly prepared, kept under constant magnetic stirring (about 500 rpm/min), was subjected to irradiation by immersing the lamp in the

reactor, fixed at the central axis of the reactor. The reactor light path was 1.8 cm. The lamp was previously heated for about 20 min and then placed in the cylindrical quartz tube. Temperature monitoring during the reactions showed a constant value so it was not necessary to refrigerate the reactor for temperature control of the reaction solution. As for the UV/TiO₂ experiments a concentration of 100 mg/L for both TiO₂ Degussa P25 and nano-sized TiO₂ photocatalyst was tested. Before photocatalytic experiments, the dried TiO₂ supported on SWCNTs underwent to a conditioning step, by carrying out a “blank” photocatalytic test (in ultrapure water) to remove remaining low amount of organic carbon. During such a test the Total Organic Carbon (TOC) concentration was measured at scheduled time intervals by a Shimadzu TOC-5050 instrument. It was found an initial TOC increase (1 mg/L) and then a reduction down to a value of about 0.4 mg/L at prolonged exposure time. The water was then removed and the aqueous solution containing the organic pollutants to be tested was poured into the reactor. This procedure guaranteed that any further residual TOC eventually leached from the photocatalyst would have been much lower than the TOC due to the organic pollutants. Furthermore, for the test performed in real wastewater, any further residual TOC eventually leached from the catalyst would have had an even lower influence. In order to evaluate if there is any adsorption of the target compounds on the photocatalyst surface, before the start of the reaction, the solution was left under stirring in the presence of the photocatalyst for about 30 minutes while protecting the reactor from the ultraviolet exposure.

Simulated solar-based photocatalytic reactions were performed by a Solar Box 1500e (Co.Fo.Megra, Milan, Italy) equipped with Xe lamp (1500 W), having an emission spectrum between 320 and 700 nm and matching the solar spectrum, operating at a fluence rate of 0.10 W/cm². Reactions were performed in a close 0.6 L cylindrical borosilicate reactor, of 155±5 mm of diameter and 30±5 mm of height with magnetic stirring.

3. Results and discussion

3.1 SWCNT/TiO₂ synthesis and characterization

TiO₂ nanocrystals were synthesized by suitably modifying a reported approach to obtain anatase TiO₂ nanorod (NR). The nucleation of TiO₂ is promoted by hydrolysis of TTIP catalyzed by TMAO exploiting OLEA as both solvent and capping agent to prevent NR from aggregation [38]. Herein the synthetic procedure was modified dispersing SWCNTs in the reaction mixture by sonication to promote the nucleation of TiO₂ at SWCNTs surface. The reaction was carried out for 5 days to first promote nucleation in anatase phase and then to allow TiO₂ surface reconstruction. The reaction

product was recovered by adding a non-solvent (ethanol or methanol) with subsequent centrifugation. Remarkably the obtained gray powder was found dispersible in nonpolar solvents (chloroform, hexane, and toluene) leading to optically clear dispersions, whereas pristine SWCNT are not dispersible in any solvent. Bare TiO₂ nanocrystals possibly nucleated far-off the SWCNTs/TiO₂ heterostructures were separated by centrifuging the obtained organic dispersion without adding any precipitating agent. Indeed, due to their low weight, bare TiO₂ nanocrystals did not precipitate, being stable in the solvent, even upon centrifugation. On the other hand a grey powder was collected at the bottom of the tube and has been re-dispersed in organic solvents after the centrifugation cycle. Such a powder has finally resulted formed of SWCNTs/TiO₂ heterostructures, as clearly pointed out by TEM and SEM investigation.

Prior to TEM and SEM analyses the SWCNTs/TiO₂ heterostructures was washed several time (5-10 times) according to the above described non-solvent precipitation procedure to remove the excess of OLEA. TEM and SEM micrographs (Figure 1) show TiO₂ NRs (19 x 3 nm; standard deviation 6%) grown onto SWCNT surface. TiO₂ NRs were found to randomly grow onto the SWCNT surface both horizontally, i.e. along the long side of the rod in contact with SWCNTs, or vertically with respect to SWCNT surface, i.e. with NRs tip in contact with SWCNTs. SEM micrographs of a typical SWCNT bundle show that the SWCNT surface is completely covered by TiO₂ NRs. SEM images clearly evidences a close packed arrangement of TiO₂ nanocrystals around SWCNTs. Such an arrangement is an extremely relevant feature, as may favor an efficient charge transfer among TiO₂ NRs [39, 40]. The mechanism behind the growth of TiO₂ NRs and dots was already reported in details in literature [38]. Rod formation is typically based on anisotropic crystal growth which can occur when surface free energy of the various crystallographic planes differs significantly, thus favoring growth along one specific direction, or, alternatively, when the growth of certain crystallographic planes is somehow prevented. In the case of TiO₂ NR growth promoted by TTIP hydrolysis, the unidirectional growth can be ascribed to the formation of complex between OLEA and TTIP, titanium oxocarboxyalkoxide, which is intrinsically anisotropic. The injection of large amount of water promote the unidirectional grow of TiO₂ according to hydrolysis of such precursor. SWCNTs could act as nucleation seeds for TiO₂ since the activation energy needed to enlarge pre-existing particles in a solution (i.e. heterogeneous nucleation/growth) is considerably lower than the barrier for the generation of novel nuclei (i.e. homogeneous nucleation) [41]. Therefore it is reasonable to propose that TiO₂ nucleation preferentially occurs at SWCNT surface. At this stage the reaction proceed toward the anisotropic growth according to the reaction path already described in literature [38]. Due to the large amount of OLEA coordinated TiO₂ nanocrystals grown on SWCNT surfaces, the as-prepared SWCNTs/TiO₂ show a dispersibility in organic solvents similar to that of TiO₂ nanocrystals.

Concomitantly, the micrometric size of the SWCNTs (5 μ m) allows to easy recovery the heterostructures by centrifugation without adding any precipitating agents.

3.2 Direct photolysis of investigate pollutants by UV and simulated solar light

During photocatalytic degradation of organic pollutants in water two main degradation mechanisms occur simultaneously, namely the photolysis and oxidation resulting from the production of HO \cdot generated by the hole/electron pair of the semiconductor. Thus, preliminary experiments were performed by photolysis. Specifically, photolysis experiments of a mixture containing the 22 investigated organic pollutants were performed by both UV and simulated solar light (Xe lamp), without any matrix (ultrapure water) and with a real water matrix (secondary wastewater effluent). Experiments were performed with organic pollutants concentration between 200 and 500 μ g L $^{-1}$. Results showed that in both ultrapure water and real secondary wastewater effluent the UV decay of all investigated pollutants follows first order kinetics. The measured first order kinetic constants are listed in Table S3 of the supporting information. Degradation experiments performed with the UV light showed that without any water matrix a relevant decay was obtained for most of the pollutants. In real secondary wastewater effluent a reduction of the degradation rate up to 90 % was observed for most pollutants, however, for a restricted number of them, namely terbutaline, BP-2 and mefenamic acid, an enhancement was observed likely due to a photosensitizer effect of the wastewater matrix.

Degradation experiments performed with the simulated solar light and without any water matrix showed much slower degradation rates being the decrease between 88 and 100 %. Beside, in real secondary wastewater effluent the simulated solar light showed to practically hinder the degradation of two organic pollutants, namely diclofenac and acetaminophen. For the remaining compounds a general enhancement of the degradation rate was found due to a photosensitizer effect of the wastewater matrix. However, the degradation rates remained much slower than those obtained employing UV light. It follows that the employment of the photocatalyst results to be crucial for the treatment under simulated solar light in order to obtain a suitable degradation of the target pollutants. In addition, it is worth noting that degradation efficiency decreased when every pollutant is investigated in the presence of the other organics with respect to the decay observed for a solution prepared with a single pollutant. A typical example of such a finding is depicted in figure 2 for warfarin. Such a behavior is likely due to the fact that when performing photolytic degradation with a mixture of pollutants the boundary conditions of photolytic degradation are not met and a slower degradation rate is consequently observed. Therefore, it is necessary to stress that it is fundamental

to perform degradation reactions in conditions approaching real situations since idealized conditions that are employed in most of the work reported in the literature do not permit easy translation of results to more practical engineered treatment operations.

3.3 Photocatalytic degradation of investigate pollutants under UV light

Photocatalytic degradations of the investigated mixture of organic pollutants followed the kinetic model of Langmuir-Hinshelwood showing first-order kinetics in both ultrapure water and real secondary wastewater effluent. Figure 3 shows the first-order kinetic constants measured during photocatalytic treatments (UV light and ultrapure water) of investigated organic pollutants employing both nano-sized TiO₂ supported on SWCNTs and conventional suspended photocatalysts TiO₂ Degussa P25. Figure 3 demonstrates that the photocatalytic efficiency of the two photocatalysts is not the same for all investigated organic pollutants. Specifically, nano-sized TiO₂ supported on SWCNTs is much more effective than conventional Degussa P25 for degradation of iopamidol, iopromide, diatrizoic acid, diclofenac, triclosan and sulfamethoxazole. For the remaining organics the degradation rates are comparable being in most of the cases Degussa P25 slightly more effective than nano-sized TiO₂ supported on SWCNTs. However, since the nano-sized TiO₂ supported on SWCNTs is in a much lower amount than the Degussa P25 TiO₂ used as a comparison, the new prepared photocatalyst presents a quite high specific efficiency. In addition, the TiO₂ supported onto CNT offers a further advantage since can be easily removed from the aqueous solution by a mild centrifugation or a filtration step and, consequently, can be reused for subsequent batch of photocatalytic treatment. Indeed, the performance of the photocatalyst during repeated reactions is an issue and was evaluated, too. Specifically, five repeated tests were carried out with a mixture of five selected organics (ibuprofen, iopromide, carbamazepine, Sulfamethoxazole and warfarin). Results showed that first order kinetic constant of ibuprofen decreased by 22% while those of the other organics remaining practically the same (Figure S3 of the supporting information).

Degradation experiments were also carried out in real secondary wastewater effluent and the measured first order kinetic constants are depicted in figure 4. The reported data clearly point out that also for UV light driven photocatalysis a general reduction of the degradation rate was obtained with respect to reactions performed in ultrapure water for both photocatalysts. In particular, such a reduction was found being for Degussa P25 between 9 and 87 % and only for estriol no difference of the degradation rate was observed. Conversely, for iopamidol, iopromide, diatrizoic acid and terbutaline a photosensitizing effect of the wastewater could be considered responsible of an increase in the degradation rate between 1.5 and 3.4 times. For the nano-sized TiO₂ supported on SWCNTs

the reduction of the degradation rate was between 9 and 96 %. The particularly severe detrimental effect of the wastewater matrix was observed for eight pollutants with both photocatalysts (right panel of figure 4). The photosensitizing effect of the wastewater in the case of the nano-sized TiO₂ supported on SWCNTs was observed only for terbutaline and β -Estradiol and was 11 and 85 %, respectively. Overall, a detrimental effect of the real wastewater matrix on the degradation efficiency can be confirmed for both the investigated photocatalysts.

Interestingly figure 4 indicates also that the kinetic constants obtained for nano-sized TiO₂ supported on SWCNTs and conventional suspended photocatalysts TiO₂ Degussa P25 catalyzed reactions are of the same order of magnitude. In particular, the marked differences obtained for reactions carried out in ultrapure water for seven pollutants (iopamidol, iopromide, diatrizoic acid, diclofenac sodium salt, triclosan and sulfamethoxazole) were not detected in real wastewater effluent. Just for diclofenac for nano-sized TiO₂ supported on SWCNTs a 30 % higher efficiency was observed. Therefore the whole ensemble of obtained data confirms the potential of nano-sized TiO₂ supported on SWCNTs also when employing real wastewater effluent.

3.4 Photocatalytic degradation of investigate pollutants under simulated solar light

Figure 5 shows the first order kinetic constants measured during photocatalytic treatments (solar light and ultrapure water) of investigated organic pollutants employing both nano-sized TiO₂ supported on SWCNTs and conventional suspended photocatalysts TiO₂ Degussa P25. From figure 5 it is evident that Degussa P25 is more effective than nano-sized TiO₂ supported on SWCNTs being the rates obtained with latter photocatalyst between 3 and 49 % those obtained with the conventional Degussa P25.

Degradation experiments were also carried out in real secondary wastewater effluent and the measured first order kinetic constants are depicted in figure 6. The reported results indicate, similarly to what found for photocatalysis employing UV light, a general reduction of the degradation rate with respect to reactions performed in ultrapure water for both photocatalysts. However, such a reduction was much higher for the Degussa P25 photocatalyst. Specifically, such a reduction was 53 % for terbutaline and for the remaining organics ranged between 87 and 99 %. For the nano-sized TiO₂ supported on SWCNTs, instead, for five organics, namely terbutaline, 2-phenyl-5-benzimidazole, BP-1, triclosan and metoprolol, a photosensitizing effect of the wastewater was observed to induce an increase the degradation rate between 14 % and 17 times. For the remaining pollutants the reduction of the degradation rates was between 11 and 98 %. Therefore, the comparison of the efficiency of the two photocatalysts in real secondary wastewater effluent clearly shows, in figure 6,

that nano-sized TiO₂ supported on SWCNTs present a higher reaction ratio rate for two pollutants, namely 2-phenyl-5-benzimidazole and BP-1 (36 and 68 %, respectively) while for six compounds, namely diatrizoic acid, terbutaline, BP-4, BP-2, β-estradiol, estriol, basically the same degradation ratio was observed. For the remaining pollutants nano-sized TiO₂ supported on SWCNTs was between 21 and 84 % less efficient than Degussa P25. Therefore, under simulated solar light irradiation, although a detrimental effect of the real wastewater matrix on the degradation efficiency can be demonstrated, such an effect was found moderate for nano-sized TiO₂ supported on SWCNTs.

4. Conclusions

A new photocatalyst based on nano-sized TiO₂ supported on SWCNTs was tested for the photocatalytic degradation, under both UV and simulated solar light, of a mixture of 22 organic pollutants in both ultrapure water and secondary wastewater effluent. Results showed that when employing secondary wastewater effluent the degradation efficiency generally decreased with both photocatalysts. The nano-sized TiO₂ supported on SWCNTs under UV irradiation displayed comparable degradation rates with respect to convention Degussa P25, while under simulated solar irradiation the new prepared photocatalyst showed slightly lower efficiency than Degussa P25. However, the proposed nano-sized TiO₂ supported on SWCNTs, contains a much lower absolute amount of TiO₂ than Degussa P25, therefore, considering also the advantage that can be easily removed from the aqueous solution by a mild centrifugation or a filtration step and, consequently, can be reused for a further photocatalytic treatment batch, the novel photocatalysts can be regard as very effective.

In addition, under simulated solar light irradiation, although a detrimental effect of the real wastewater matrix on the degradation efficiency can be demonstrated, such an effect was found moderate for nano-sized TiO₂ supported on SWCNTs. The obtained results indicates that, while it is fundamental to perform degradation reactions in conditions approaching real situations, since idealized conditions that are employed in most of the work reported in the literature do not allow an easy translation of results to real engineered treatment operations,

Overall, the obtained results showed that proposed photocatalyst based on nano-sized TiO₂ supported on SWCNTs has proved to be a promising candidate, thanks to its unique optoelectronic properties, electronic to be used in a photocatalytic based-AOP and to be integrated with a biological step for the effective removal of emerging organic pollutants.

Acknowledgements

This work was partially supported by the EC-funded 7th FP Project LIMPID (Grant No. 310177), and by the Italian Ministry of Foreign Affairs, in the framework of the activities foreseen by the Agreement on industrial, scientific and technological research and development cooperation between Italy and Israel, funding the project “Degradation of recalcitrant pharmaceuticals in municipal wastewater by advanced oxidation processes”.

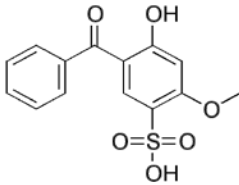
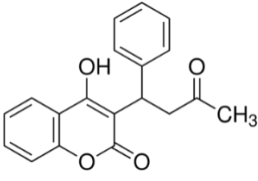
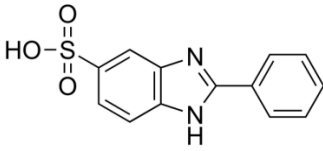
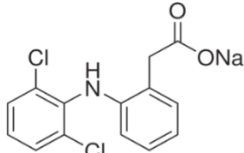
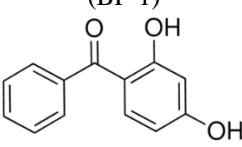
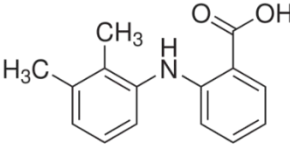
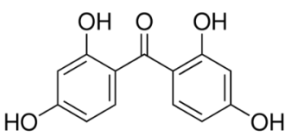
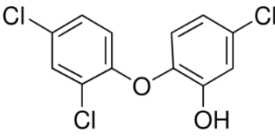
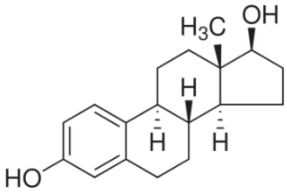
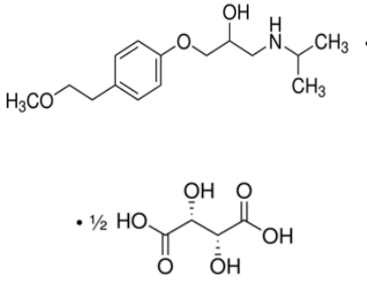
References

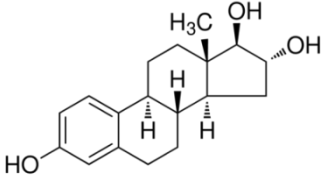
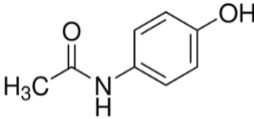
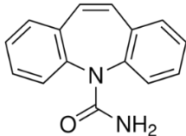
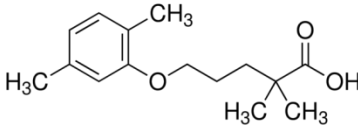
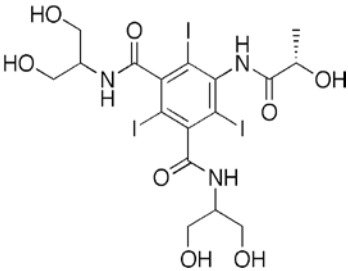
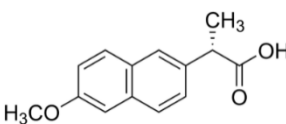
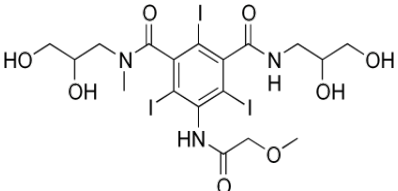
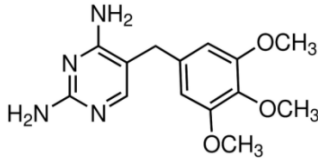
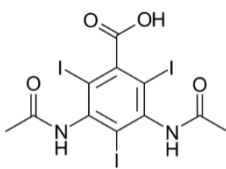
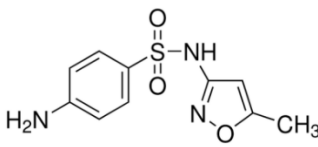
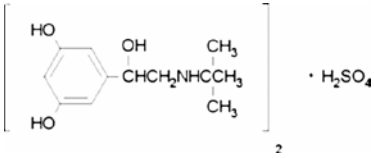
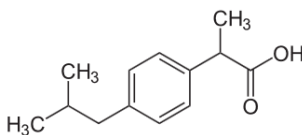
- [1] N. Ratola, A. Cincinelli, A. Alves and A. Katsoyiannis, *J. Hazard. Mater.*, 239–240 (2012) 1.
- [2] N. De la Cruz, R.F. Dantas, J. Giménez and S. Esplugas, *Appl. Catal. B-Environ.*, 130–131 (2013) 249.
- [3] A. Bernabeu, R.F. Vercher, L. Santos-Juanes, P.J. Simón, C. Lardín, M.A. Martínez, J.A. Vicente, R. González, C. Llosá, A. Arques and A.M. Amat, *Catal. Today*, 161 (2011) 235.
- [4] E.Z. Harrison, S.R. Oakes, M. Hysell and A. Hay, *Sci. Total Environ.*, 367 (2006) 481.
- [5] C.A. Kinney, E.T. Furlong, S.D. Zaugg, M.R. Burkhardt, S.L. Werner, J.D. Cahill and G.R. Jorgensen, *Environ. Sci. Technol.*, 40 (2006) 7207.
- [6] S. Carbonaro, M.N. Sugihara and T.J. Strathmann, *Appl. Catal. B-Environ.*, 129 (2013) 1.
- [7] N. Klammerth, L. Rizzo, S. Malato, M.I. Maldonado, A. Agüera and A.R. Fernández-Alba, *Water Res.*, 44 (2010) 545.
- [8] E.K. Muirhead, A.D. Skillman, S.E. Hook and I.R. Schultz, *Environ. Sci. Technol.*, 40 (2005) 523.
- [9] M. DeLorenzo and J. Fleming, *Arch. Environ. Contam. Toxicol.*, 54 (2008) 203.
- [10] J.E. Drewes and S. Khan, in J. Edzwald (Editor), *Water Quality and Treatment*, 6th Edition, American Water Works Association, Denver, Colorado., 2011, p. 48.
- [11] J.-M. Herrmann, *Appl. Catal. B-Environ.*, 99 (2010) 461.
- [12] M. Sievers, in P. Wilderer (Editor), *Treatise on Water Science*, Elsevier, Oxford, 2011, p. 377.
- [13] A. Lopez, A. Bozzi, G. Mascolo and J. Kiwi, *Journal of Photochemistry and Photobiology a-Chemistry*, 156 (2003) 121.
- [14] P. Raja, A. Bozzi, W.F. Jardim, G. Mascolo, R. Renganathan and J. Kiwi, *Applied Catalysis B-Environmental*, 59 (2005) 249.

- [15] M.A. Sousa, C. Gonçalves, V.J.P. Vilar, R.A.R. Boaventura and M.F. Alpendurada, *Chem. Eng. J.*, 198–199 (2012) 301.
- [16] M.N. Sugihara, D. Moeller, T. Paul and T.J. Strathmann, *Appl. Catal. B-Environ.*, 129 (2013) 114.
- [17] L. Prieto-Rodríguez, S. Miralles-Cuevas, I. Oller, A. Agüera, G.L. Puma and S. Malato, *J. Hazard. Mater.*, 211–212 (2012) 131.
- [18] M. Pelaez, N.T. Nolan, S.C. Pillai, M.K. Seery, P. Falaras, A.G. Kontos, P.S.M. Dunlop, J.W.J. Hamilton, J.A. Byrne, K. O'Shea, M.H. Entezari and D.D. Dionysiou, *Appl. Catal. B-Environ.*, 125 (2012) 331.
- [19] A. Mitsionis, T. Vaimakis, C. Trapalis, N. Todorova, D. Bahnemann and R. Dillert, *Appl. Catal. B-Environ.*, 106 (2011) 398.
- [20] D. Šojić, V. Despotović, B. Abramović, N. Todorova, T. Giannakopoulou and C. Trapalis, *Molecules*, 15 (2010) 2994.
- [21] Á. Anglada, A. Urtiaga, I. Ortiz, D. Mantzavinos and E. Diamadopoulos, *Water Res.*, 45 (2011) 828.
- [22] A. Detomaso, G. Mascolo and A. Lopez, *Rapid Commun. Mass Spectrom.*, 19 (2005) 2193.
- [23] L.A. Ioannou, E. Hapeshi, M.I. Vasquez, D. Mantzavinos and D. Fatta-Kassinos, *Solar Energy*, 85 (2011) 1915.
- [24] A. Katsoni, H.T. Gomes, L.M. Pastrana-Martínez, J.L. Faria, J.L. Figueiredo, D. Mantzavinos and A.M.T. Silva, *Chem. Eng. J.*, 172 (2011) 634.
- [25] M. Klavarioti, D. Mantzavinos and D. Kassinos, *Environ. Int.*, 35 (2009) 402.
- [26] R. Comparelli, E. Fanizza, M.L. Curri, P.D. Cozzoli, G. Mascolo and A. Agostiano, *Appl. Catal. B-Environ.*, 60 (2005) 1.
- [27] N. Miranda-García, S. Suárez, B. Sánchez, J.M. Coronado, S. Malato and M.I. Maldonado, *Appl. Catal. B-Environ.*, 103 (2011) 294.
- [28] G. Mascolo, R. Comparelli, M.L. Curri, G. Lovecchio, A. Lopez and A. Agostiano, *J. Hazard. Mater.*, 142 (2007) 130.
- [29] R. Comparelli, P.D. Cozzoli, M.L. Curri, A. Agostiano, G. Mascolo and G. Lovecchio, *Water Sci. Technol.*, 49 (2004) 183.
- [30] N. De la Cruz, J. Giménez, S. Esplugas, D. Grandjean, L.F. de Alencastro and C. Pulgarín, *Water Res.*, 46 (2012) 1947.
- [31] R. Leary and A. Westwood, *Carbon*, 49 (2011) 741.
- [32] J.L. de Morais and P.P. Zamora, *J. Hazard. Mater.*, 123 (2005) 181.

- [33] A. Zapata, I. Oller, L. Rizzo, S. Hilgert, M.I. Maldonado, J.A. Sánchez-Pérez and S. Malato, *Appl. Catal. B-Environ.*, 97 (2010) 292.
- [34] N. Klammerth, L. Rizzo, S. Malato, M.I. Maldonado, A. Agüera and A.R. Fernández-Alba, *Water Res.*, 44 (2010) 545.
- [35] N. Klammerth, S. Malato, M.I. Maldonado, A. Agüera and A.R. Fernández-Alba, *Environ. Sci. Technol.*, 44 (2010) 1792.
- [36] L. Prieto-Rodríguez, D. Spasiano, I. Oller, I. Fernández-Calderero, A. Agüera and S. Malato, *Catal. Today*, 209 (2013) 188.
- [37] C. Di Iaconi, G. Del Moro, M. De Sanctis and S. Rossetti, *Water Res.*, 44 (2010) 3635.
- [38] P.D. Cozzoli, A. Kornowski and H. Weller, *JACS*, 125 (2003) 14539.
- [39] A.A. Ismail, D.W. Bahnemann, I. Bannat and M. Wark, *J. Phys. Chem. C*, 113 (2009) 7429.
- [40] F. Petronella, S. Diomede, E. Fanizza, G. Mascolo, T. Sibillano, A. Agostiano, M.L. Curri and R. Comparelli, *Chemosphere*, 91 (2013) 941.
- [41] M. Casavola, R. Buonsanti, G. Caputo and P.D. Cozzoli, *Eur. J. Inorg. Chem.*, 2008 (2008) 837.

Table 1. Investigated PPCPs.

| Analyte | Category /Use | Analyte | Category /Use |
|---|--|---|--|
| <p>5-Benzoyl-4-hydroxy-2-methoxy benzenesulfonic acid (BP-4)</p>  <p>CAS 4065-45-6</p> | <p>UV Filter Personal care product</p> | <p>Warfarin</p>  <p>CAS 81-81-2</p> | <p>Pharmaceutical Anticoagulant</p> |
| <p>2-Phenyl-5-benzimidazole sulfonic acid</p>  <p>CAS 27503-81-7</p> | <p>UV Filter Personal care product</p> | <p>Diclofenac sodium salt</p>  <p>CAS 15307-79-6</p> | <p>Pharmaceutical Anti-inflammatory</p> |
| <p>2,4-Diidrossi-benzophenone (BP-1)</p>  <p>CAS 131-56-6</p> | <p>UV Filter Personal care product</p> | <p>Mefenamic acid</p>  <p>CAS 61-68-7</p> | <p>Pharmaceutical Anti-inflammatory, analgesic, antipyretic</p> |
| <p>2,2',4,4' Tetrahydroxybenzophenone (BP-2)</p>  <p>CAS 131-55-5</p> | <p>UV Filter Personal care product</p> | <p>Triclosan</p>  <p>CAS 3380-34-5</p> | <p>Pharmaceutical Antimicrobial</p> |
| <p>β-Estradiol (E2)</p>  <p>CAS 50-28-2</p> | <p>Endocrine disruptor</p> | <p>(\pm)-Metoprolol (+)-tartrate salt</p>  <p>CAS 56392-17-7</p> | <p>Pharmaceutical β_1 receptor blocker used in hypertension</p> |

| Analyte | Category /Use | Analyte | Category /Use |
|--|---|--|--|
| <p>Estriol (E3)</p>  <p>CAS 50-27-1</p> <p>Carbamazepine</p> | Endocrine disruptor | <p>Acetaminophen</p>  <p>CAS 103-90-2</p> <p>Gemfibrozil</p> | <p>Pharmaceutical</p> <p>Analgesic, antipyretic</p> |
|  <p>CAS 298-46-4</p> <p>Iopamidol</p> | <p>Pharmaceutical</p> <p>Psycholeptics</p> |  <p>CAS 25812-30-0</p> <p>Naproxene</p> | <p>Pharmaceutical</p> <p>Drug used to lower lipid levels</p> |
|  <p>CAS 60166-93-0</p> <p>Iopromide</p> | <p>Pharmaceutical</p> <p>X-ray contrast media</p> |  <p>CAS 22204-53-1</p> <p>Trimethoprim</p> | <p>Pharmaceutical</p> <p>Anti-inflammatory, analgesic, antipyretic</p> |
|  <p>CAS 73334-07-3</p> <p>Diatrizoate</p> | <p>Pharmaceutical</p> <p>X-ray contrast media</p> |  <p>CAS 738-70-5</p> <p>Sulfamethoxazole</p> | <p>Pharmaceutical</p> <p>Antibiotic</p> |
|  <p>CAS 117-96-4</p> <p>Terbutaline hemisulfate salt</p> | <p>Pharmaceutical</p> <p>X-ray contrast media</p> |  <p>CAS 723-46-6</p> <p>Ibuprofen</p> | <p>Pharmaceutical</p> <p>Antibiotic</p> |
|  <p>Pharmaceutical</p> <p>β_2-adrenergic receptor agonist used as bronchodilator</p> | <p>Pharmaceutical</p> <p>Anti-inflammatory</p> |  | |

| Analyte | Category /Use | Analyte | Category /Use |
|----------------|---------------|----------------|---------------|
| CAS 23031-32-5 | | CAS 15687-27-1 | |

Table 2. Characteristics of the employed real secondary effluent

| Parameter | Value |
|--|----------------|
| Conductivity | 874 μ S/cm |
| Total suspended solids (SST) | 24 mg/L |
| Chemical Oxygen Demand (COD) | 51 mg/L |
| Ammonia nitrogen (N-NH ₄ ⁺) | 11 mg/L |
| Nitrates (N-NO ₃ ⁻) | 46 mg/L |
| Nitrites (N-NO ₂ ⁻) | 1.7 mg/L |
| TN | 67 mg/L |

Figure captions

- Figure 1. Scanning (a) and Transmission (b) electron microscopy images of SWCNTs/TiO₂ heterostructures. SEM micrography has been obtained by in-lens SE detector. The SEM measurements have been performed with an accelerating voltage of 1kV, a working distance of 1.6 mm and an aperture size of 30 μm.
- Figure 2. Warfarin degradation by UV photolysis and UV photocatalysis employing conventional suspended catalysts TiO₂ Degussa P25 in ultrapure water. Warfarin dissolved as a single compound (left) and as a mixture together with the other investigated pollutants (right).
- Figure 3. First order kinetic constants (*k*) of UV photocatalytic treatments for the investigated organic pollutants employing both nano-sized TiO₂ supported on SWCNTs and conventional suspended catalysts TiO₂ Degussa P25 in ultrapure water. Initial catalyst concentration 100 mg L⁻¹.
- Figure 4. First order kinetic constants (*k*) of UV photocatalytic treatments for the investigated organic pollutants employing both nano-sized TiO₂ supported on SWCNTs and conventional suspended catalysts TiO₂ Degussa P25 in real secondary wastewater effluent. Initial catalyst concentration 100 mg L⁻¹. For β-estradiol and acetaminophen the solubility in the wastewater was below the instrumental detection limit (80 μg L⁻¹).
- Figure 5. First order kinetic constants (*k*) of simulated solar light photocatalytic treatments for the investigated organic pollutants employing both nano-sized TiO₂ supported on SWCNTs and conventional suspended catalysts TiO₂ Degussa P25 in ultrapure water. Initial catalyst concentration 100 mg L⁻¹.
- Figure 6. First order kinetic constants (*k*) of simulated solar light photocatalytic treatments for the investigated organic pollutants employing both nano-sized TiO₂ supported on SWCNTs and conventional suspended catalysts TiO₂ Degussa P25 in real secondary wastewater effluent. Initial catalyst concentration 100 mg L⁻¹. For β-estradiol and acetaminophen the solubility in the wastewater was below the instrumental detection limit (80 μg L⁻¹).

Figure 1

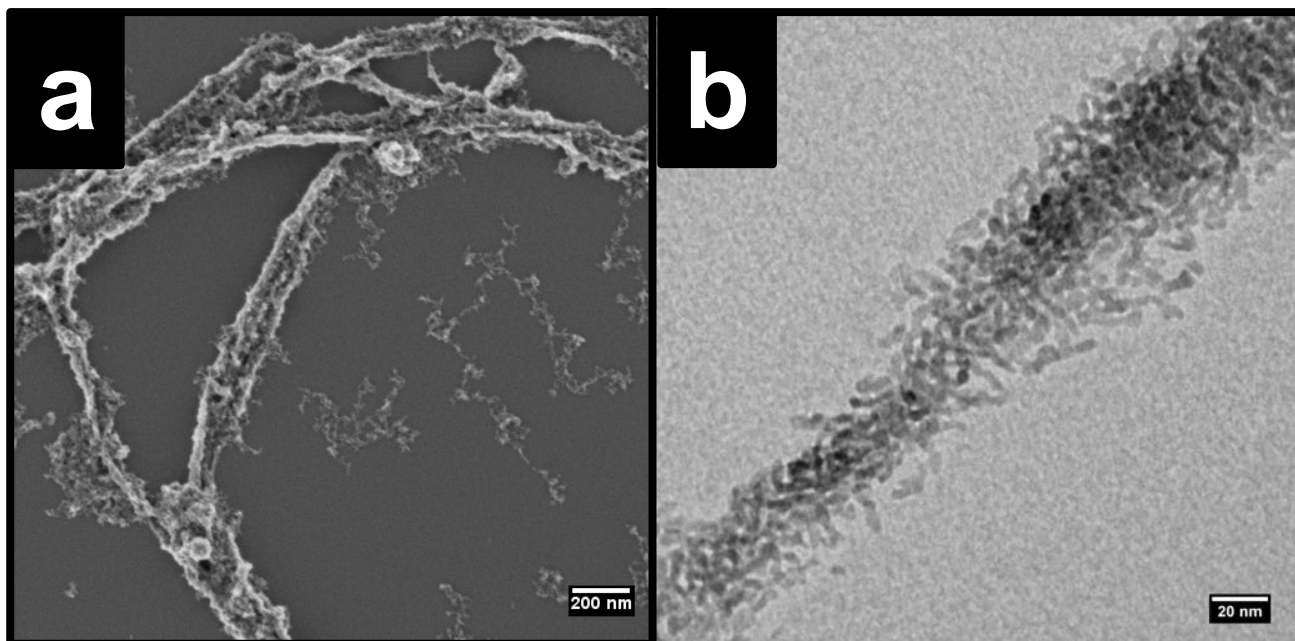


Figure 1. Scanning (a) and Transmission (b) electron microscopy images of SWCNTs/TiO₂ heterostructures. SEM micrography has been obtained by in-lens SE detector. The SEM measurements have been performed with an accelerating voltage of 1kV, a working distance of 1.6 mm and an aperture size of 30 μ m.

Figure 2

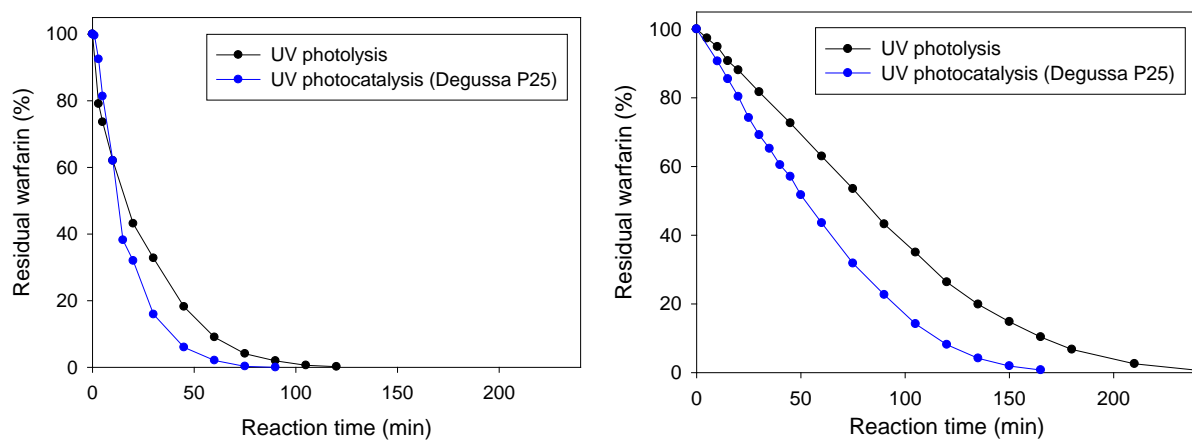


Figure 2. Warfarin degradation by UV photolysis and UV photocatalysis employing conventional suspended catalysts TiO₂ Degussa P25 in ultrapure water. Warfarin dissolved as a single compound (left) and as a mixture together with the other investigated pollutants (right).

Figure 3

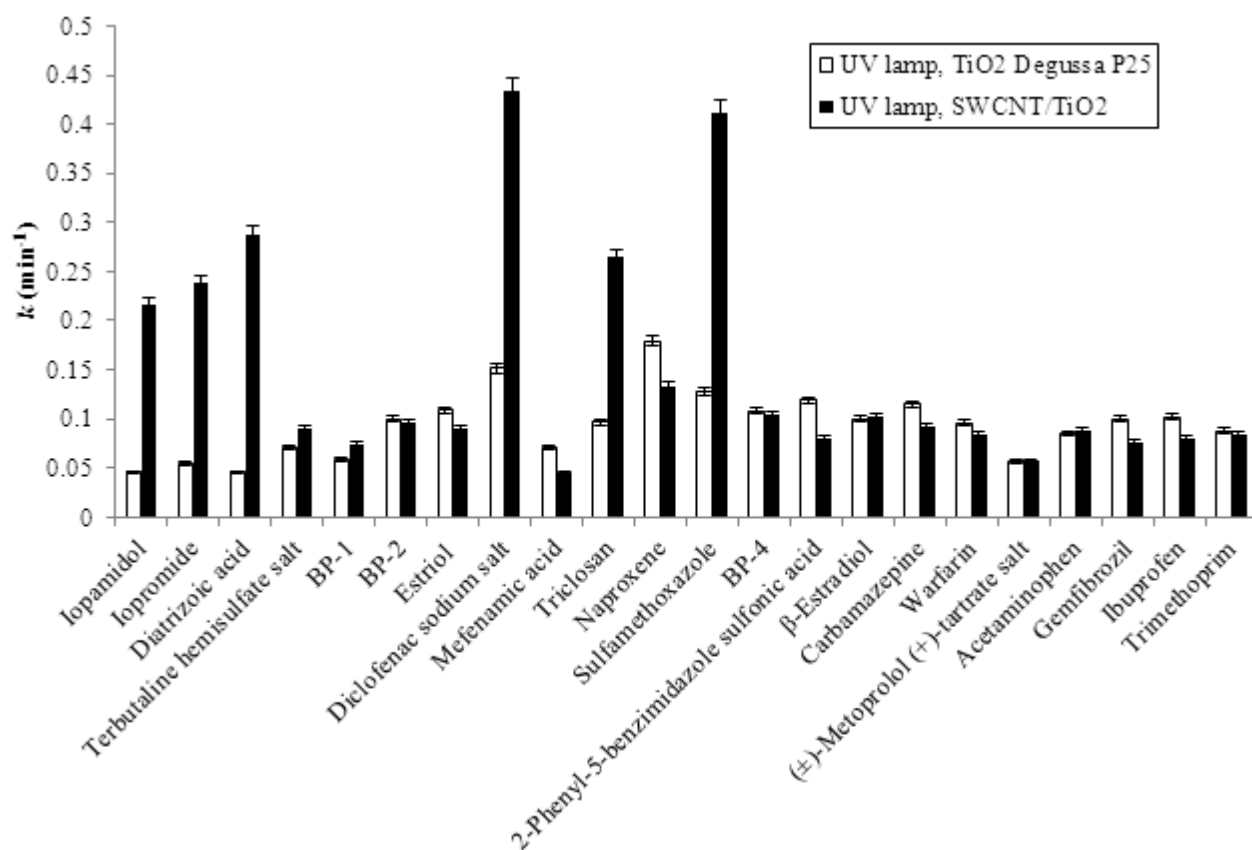


Figure 3. First order kinetic constants (k) during UV photocatalytic treatments for the investigated organic pollutants employing both nano-sized TiO₂ supported on SWCNTs and conventional suspended catalysts TiO₂ Degussa P25 in ultrapure water. Initial catalyst concentration 100 mg L⁻¹.

Figure 4

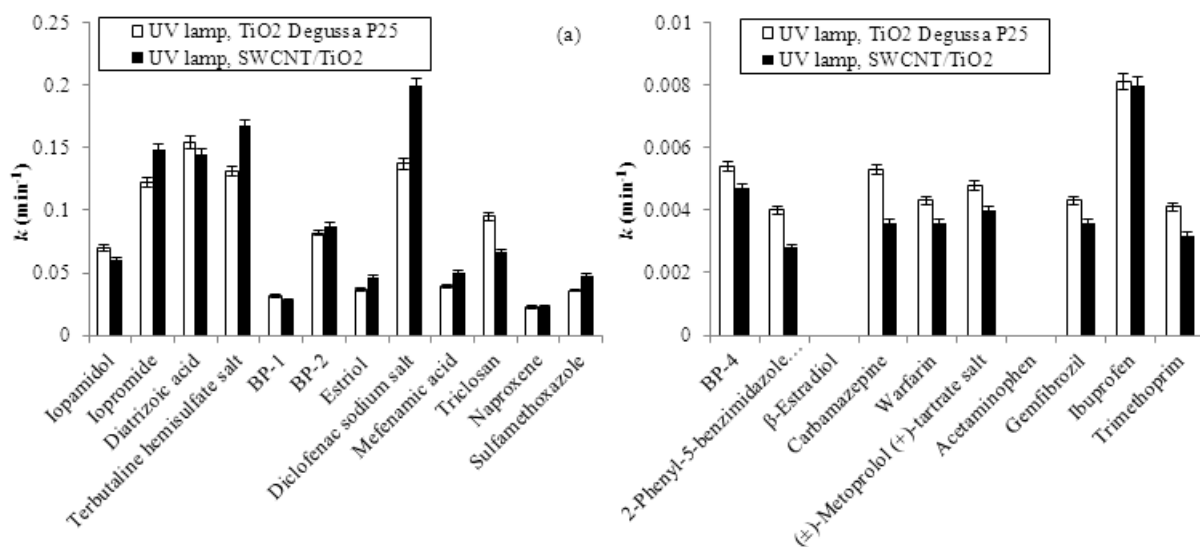


Figure 4. First order kinetic constants (k) during UV photocatalytic treatments for the investigated organic pollutants employing both nano-sized TiO₂ supported on SWCNTs and conventional suspended catalysts TiO₂ Degussa P25 in real secondary wastewater effluent. Initial catalyst concentration 100 mg L⁻¹. For β -estradiol and acetaminophen the solubility in the wastewater was below the instrumental detection limit (80 $\mu\text{g L}^{-1}$).

Figure 5

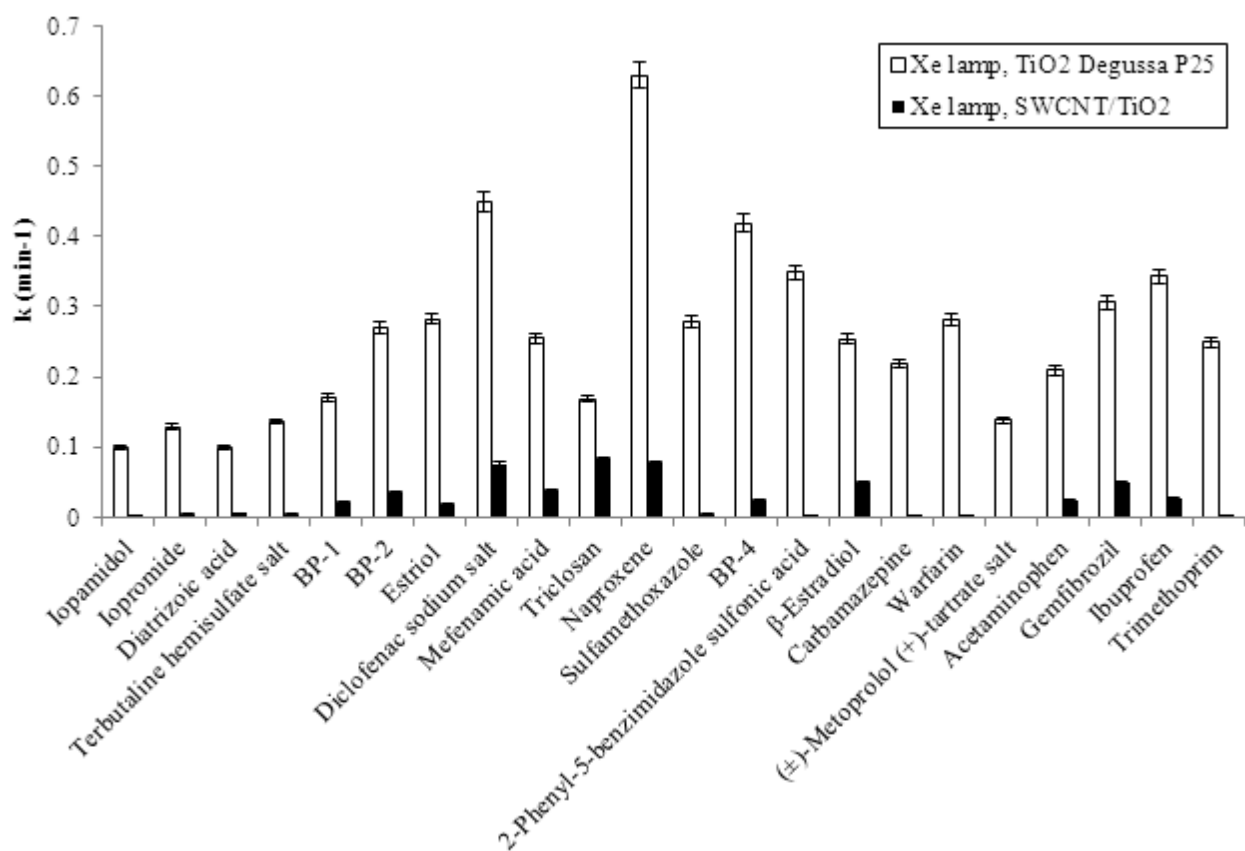


Figure 5. First order kinetic constants (k) during simulated solar light photocatalytic treatments for the investigated organic pollutants employing both nano-sized TiO₂ supported on SWCNTs and conventional suspended catalysts TiO₂ Degussa P25 in ultrapure water. Initial catalyst concentration 100 mg L⁻¹.

Figure 6

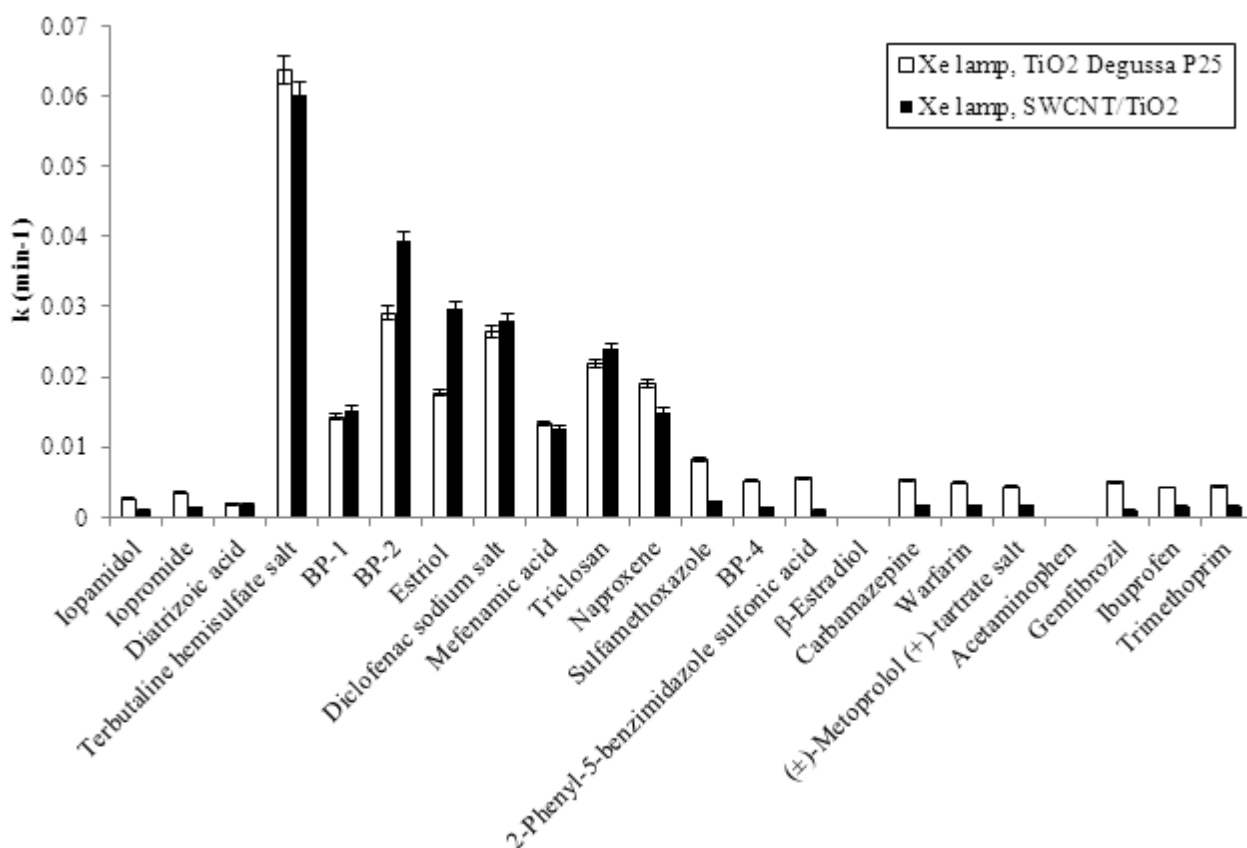


Figure 6. First order kinetic constants (k) during simulated solar light photocatalytic treatments for the investigated organic pollutants employing both nano-sized TiO₂ supported on SWCNTs and conventional suspended catalysts TiO₂ Degussa P25 in real secondary wastewater effluent. Initial catalyst concentration 100 mg L⁻¹. For β -estradiol and acetaminophen the solubility in the wastewater was below the instrumental detection limit (80 μ g L⁻¹).